

The default mode network integrity in patients with Parkinson's disease is levodopa equivalent dose-dependent

L. Krajcovicova · M. Mikl · R. Marecek ·
Irena Rektorova

Received: 8 July 2011 / Accepted: 28 September 2011
© Springer-Verlag 2011

Abstract Disturbances in the default mode network (DMN) have been described in many neurological and psychiatric disorders including Parkinson's disease (PD). The DMN is characterized by basal activity that increases during rest or passive visual fixation and decreases ("deactivates") during cognitive tasks. The network is believed to be involved in cognitive processes. We examined the DMN in PD patients on dopaminergic medication with normal cognitive performance compared to age- and gender-matched healthy controls (HC) using fMRI and three methodological procedures: independent component analysis of resting-state data, analysis of deactivation during a complex visual scene-encoding task, and seed-based functional connectivity analysis. In the PD group, we also studied the effect of dopaminergic medication on the DMN integrity. We did not find any difference between the PD and HC groups in the DMN, but using the daily levodopa equivalent dose as a covariate, we observed an enhanced functional connectivity of the DMN in the posterior cingulate cortex and decreased activation in the left parahippocampal gyrus during the cognitive task. We conclude that dopaminergic therapy has a specific effect on both the DMN integrity and task-related brain activations in cognitively unimpaired PD patients, and these effects seem to be dose-dependent.

Keywords Parkinson's disease · Default mode network · Deactivation · Functional connectivity · Hippocampus · Levodopa

Introduction

In the last two decades, many studies have emerged examining an intriguing network, the function of which is not primarily to respond to external stimuli but rather to prepare reactions to these stimuli. This network is commonly known as a "resting state" network (RSN) because of its basal activity during rest or passive visual fixation. It is also characterized by typical low-frequency signal fluctuations (below 0.1 Hz) (Fox et al. 2005; Fox and Raichle 2007; Raichle and Snyder 2007; Rogers et al. 2007) and to date, approximately ten RSNs have been identified (Robinson et al. 2009; Rogers et al. 2007; Weissenbacher et al. 2009). The default mode network (DMN), as a unique part of these RSNs, differs from other RSNs in its ability to attenuate its activity during goal-directed behaviour. When a cognitive task is performed, the DMN shows itself in "deactivation". The areas that have been identified as involved in the DMN are the medial prefrontal cortex and anterior cingulate cortex (MPFC/ACC), the posterior cingulate cortex and precuneus (PCC/P), and the lateral parietal and temporal cortices, as well as medial temporal formations including the hippocampi and parahippocampi. It is assumed that the extent of the deactivation or resting-state activity reflects the ability of the brain to redirect its activity from internal to external, goal-directed processes (Gusnard et al. 2001; Raichle et al. 2001; Tomasi et al. 2009), review past knowledge, and plan future behaviours (Binder et al. 1999). Previous studies have documented that the DMN is disrupted in patients with specific

L. Krajcovicova · M. Mikl · R. Marecek · I. Rektorova
Applied Neurosciences Research Group,
Central European Institute of Technology, CEITEC,
Masaryk University, Brno, Czech Republic

L. Krajcovicova · M. Mikl · R. Marecek · I. Rektorova (✉)
First Department of Neurology, St Anne's Hospital,
School of Medicine, Masaryk University, Brno,
Czech Republic
e-mail: irena.rektorova@fnusa.cz

neurodegenerative and psychiatric diseases (e.g. dementia, schizophrenia, depression, attention deficit/hyperactivity disorders) (Bluhm et al. 2007; Broyd et al. 2009; Buckner et al. 2005; Greicius et al. 2004; Li et al. 2002; Liang et al. 2006; Liu et al. 2008; Wang et al. 2006; Zang et al. 2007; Zhou et al. 2007, 2008). The situation in patients with Parkinson's disease (PD) remains less clear, especially concerning the role of dopamine in modulating the DMN and its behavioural implications. The results of available studies seem to be rather contradictory, suggesting similarities between PD patients and healthy controls (HC) as well as specific impairments of the DMN in PD patients.

For example, in non-medicated PD patients as compared to HC, Van Eimeren et al. (2009) observed quantitative differences in deactivations during a cognitive task, specifically in the PCC/P. The authors demonstrated a reversed pattern of activation and deactivation in PCC/P for PD patients compared to HC, and the connectivity analysis showed the MPFC and caudate nucleus were functionally disconnected in PD patients. Conversely, Nagano-Saito et al. (2009) described a similar pattern of deactivation in PD patients in both ON and OFF conditions that was also comparable to that of HC. Another study comparing ON and OFF states in PD patients (Delaveau et al. 2010) showed decreased deactivation in the PCC/P, ACC, and lateral temporal and parietal cortices in non-medicated PD patients as compared to HC. After levodopa administration, the DMN integrity in PD patients was restored. Regarding the functional connectivity, Helmich et al. (2010) described decreased resting-state connectivity between the posterior putamen and the inferior parietal cortex in PD patients OFF-medication, and this region showed increased functional connectivity with the anterior putamen. Some studies have suggested that dopamine manipulation can modulate the DMN integrity in HC (Achard and Bullmore 2007; Kelly et al. 2009; Li et al. 2000; Nagano-Saito et al. 2008; Tomasi et al. 2009) in terms of decreasing the deactivation in the DMN and changing its functional connectivity.

The objective of our study was to assess the integrity of the DMN in PD patients as compared to HC by analysing resting-state data, BOLD signal decreases (deactivations) during a cognitive task, and seed functional connectivity with the seed located in PCC/P and MPFC/ACC. To evaluate brain deactivation we used a complex visual scene-encoding task (Rabin et al. 2004). This task provides a measure of episodic memory ability that taps into both verbal and non-verbal memory systems and symmetrically activates cortices extending from visual association areas rostrally to bilateral mesial temporal regions. We have previously demonstrated that this task is also suitable for examining deactivations within the DMN in HC

(Krajcovicova et al. 2010). We chose both the posterior and anterior DMN nodes as our regions of interest for the seed connectivity analysis because of previously described deficits in the deactivation of this area of the DMN in non-medicated PD patients as compared to HC (Van Eimeren et al. 2009; Delaveau et al. 2010). Additionally, we assumed the specific influence of dopaminergic therapy on the DMN integrity in our medicated PD patients. To test this hypothesis, we assessed the effect of daily levodopa equivalent dose (LED) on seed functional connectivity, deactivation, and resting-state activity.

Methods and materials

Subjects

The study consisted of 18 non-demented patients and non-depressed PD patients (Hughes et al. 1992) (8 females, 10 males; mean age 63.5 ± 9.07 , ranging from 44 to 84 years) and 18 HC (10 females, 8 males; mean age 60.8 ± 6.67 years, ranging from 46 to 77 years). Six patients had a tremor-dominant and 12 patients had akinetic-rigid form of PD. All but one patient were on dopaminergic therapy. One patient was on monoamine oxidase-B (MAO-B) inhibitor selegiline only. We enrolled right-handed subjects with at least 8 years of education. We also made efforts to match the two groups for age and gender. The history of stroke and ischaemia focus on brain imaging were exclusion criteria in our study as well as extensive white matter lesions. None of our patients met ICD-10 criteria for depression, anxiety, apathy or any other major psychiatric disease (World Health Organization 2007) and none of our PD patients took anticholinergic drugs or amantadine 4 weeks prior to and at the time of scanning. All participants were enrolled in the First Department of Neurology, Masaryk University and St. Anne's Teaching Hospital in Brno, Czech Republic.

All subjects underwent the Addenbrooke's Cognitive Examination—Revised (ACE-R) (Hummelová-Fanfrdlová et al. 2009; Mathuranath et al. 2000). ACE-R is a relatively detailed screening instrument for dementia. It consists of 18 tasks structured into 5 domains evaluating memory, verbal fluency, attention and orientation, speech, and visual-spatial abilities. The test includes the mini-mental state examination (MMSE), the result of which can be extracted from the total scores. The maximum score of ACE-R is 100 points (i.e. the best cognitive performance) and the minimum score is 0 (i.e. the worst cognitive performance). With a score of ≤ 88 points, the sensitivity for diagnosis of dementia is 94% and specificity is 89% (Mathuranath et al. 2000). We enrolled only those HC and

PD patients who scored >88 points on the ACE-R and ≥ 27 points on the MMSE (i.e. non-demented).

All PD patients were on stable dopaminergic treatment for at least 4 weeks prior to the study commencement and during the study. PD patients were scanned on medication in the “ON” state without dyskinesias, i.e. 1–2 h after their morning dose, to minimize motor artefacts (and tremor in particular) during scanning. LED was calculated for each PD patient (Parkin et al. 2002). All subjects had normal vision in order to correctly recognize the pictures seen during the scanning. Informed consent was obtained from each participant prior to the experiment. The study received the approval of the local ethics committee.

Task

The experiment comprised two parts: (1) a complex visual scene-encoding task (Rabin et al. 2004); and (2) a resting-state functional measurement. During the complex visual scene-encoding task, the subjects were instructed to view the pictures and to remember them. The encoding performance was evaluated with subsequent recognition testing. Visual stimuli were delivered to a projection screen via a data projector and were seen by the subjects through a mirror that was mounted on the MRI scanner’s radio frequency head coil. The visual task was epoch-related, with ten pictures in each epoch. We used two types of pictures: pictures representing the cognitive task itself and control images. Sixty photographs showing complex scenes (e.g. countryside, cities; see Fig. 1) were used for active periods, and 70 degraded images (a degraded image was created using one of the photographs with all of the pixels randomly altered) were used for passive periods. Seven passive epochs (P) and six active epochs (A) were intermixed in the order PAPAPAPAPAPAP. Each epoch consisted of ten photographs or degraded images. Each picture was displayed for 3,500 ms and was followed by a black screen for 600 ms. The whole task was 8 min and 53 s in length. The complex visual scene-encoding task was followed by a resting-state functional measurement lasting for 15 min. Subjects were only instructed to lie still with their eyes closed and rest, but not to fall asleep and not to think of anything particular. We verified that all PD and HC subjects had not fallen asleep during the scanning by asking them relevant questions immediately after the resting-state scanning. Approximately 30 min after the end of the fMRI cognitive task, the recognition phase of the complex visual scene-encoding task was performed in a quiet room outside the scanner. Subjects were exposed to all 60 previous visual scenes (photographs) randomly mixed with 60 new pictures (also complex scenes with similar features) as they were projected via computer monitor. The subjects were instructed to categorize each picture as “previously seen”

or “new” by pressing a corresponding button. If they could not press the buttons themselves, they were asked to respond verbally and the answers were uploaded by the examiner. The relative achievement score (in %) was calculated as follows: correctly marked previously seen + correctly marked new/all presented images. We used the Mann–Whitney *U* test to assess the significance of differences between the groups in their cognitive test results (ACE-R and recognition of the complex visual scenes).

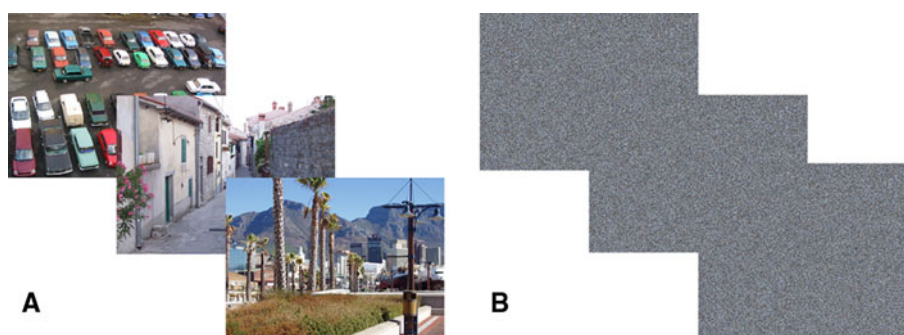
Image acquisition

Imaging was performed on a 1.5-T Siemens Symphony scanner equipped with Numaris 4 System (MRease). Functional images for the visual task were acquired using a gradient echo, echoplanar imaging (EPI) sequence: TR (scan repeat time) = 2,050 ms, TE = 50 ms, FOV = 240 mm, flip angle = 90°, matrix size 64 × 64, slice thickness = 5 mm, 20 transversal slices per scan. The imaged volume covered most of the brain excluding the vertex. Each functional measurement during the cognitive task consisted of 260 scans. The visual task was followed by a resting-state functional measurement using a gradient echo, EPI sequence: TR = 3,000 ms, TE = 40 ms, FOV = 220 mm, flip angle = 90°, matrix size 64 × 64, slice thickness = 3.5 mm, 32 transversal slices per scan. During the resting-state measurement, 300 scans were acquired. Following functional measurements, high-resolution anatomical T1-weighted images were acquired using a 3D sequence that served as a matrix for the functional imaging (160 sagittal slices, resolution 256 × 256 resampled to 512 × 512, slice thickness = 1.17 mm, TR = 1,700 ms, TE = 3.96 ms, FOV = 246 mm, flip angle = 15°). The subjects were instructed to remain still while in the scanner.

Conventional analysis of fMRI data from the complex visual scene-encoding task

An SPM5 program (Functional Imaging Laboratory, the Wellcome Department of Imaging Neuroscience, Institute of Neurology at University College London, UK) running under Matlab 7.6 (Mathworks Inc., USA) was used to analyse the fMRI data. The following pre-processing was applied to each subject’s time series of fMRI scans: realignment and unwarping of functional scans to correct for head movement; normalization to fit into a standard anatomical space (MNI); and spatial smoothing using a Gaussian filter with a FWHM of 8 mm. The voxel size generated from the above acquisition parameters was oversampled to 3 × 3 × 3 mm. To determine the brain regions that showed significantly greater activation or

Fig. 1 Examples of stimuli used for the complex visual scene-encoding task. **a** Pictures showing complex scenes (e.g. countryside, city) used for active period. **b** Control stimuli—a degraded image created using one of the photographs with all of the pixels randomly altered



deactivation with respect to active periods, a General Linear Model (GLM) as implemented in SPM5 was used. The experimental stimulation time-course was convolved with a canonical haemodynamic response function. A high-pass filter with a cut-off at 128 s and an autoregressive model to estimate serial correlations were used within the GLM. The movement parameters obtained during realignment were used as nuisance variables (regressors of no interest) in design matrix. Statistical parametric maps with *t*-statistics were computed to assess the effects of activation (BOLD signal increase) or deactivation (BOLD signal decrease) with respect to the active condition. Corresponding contrast files were carried out into the second-level analyses. We used a random-effect analysis as implemented in SPM5 to assess mean group activations/deactivations (one-sample *t* test) and differences between the groups (two-sample *t* test). Age and gender were used as covariates for these analyses. Correlation analysis between behavioural outcomes and activations/deactivations in both groups was assessed and the effects of daily LED and disease duration were assessed separately for the PD group with age and gender as covariates. Group results were assessed using cluster-level inference at $p(\text{FWE}) < 0.05$ at a height threshold of $p(\text{uncor}) < 0.001$.

Seed correlation analysis of fMRI data from complex visual scene-encoding task

Coordinates of local maxima from deactivations across both groups were selected from the PCC/P (−6, −57, 33) and MPFC/ACC (3, 39, 12), the main nodes of the DMN. Subject-specific time series were extracted as eigenvariates from spheres with a radius of 6 mm centred at these coordinates. These time series were used as regressors for functional connectivity analysis (seed correlation analysis) on data from the task. The GLM for seed correlation analysis was built as follows: the extracted time series was used as a regressor of interest accompanied by a global signal time series (calculated by SPM5 during the conventional analysis as a mean signal of each scan) and by six time series of movement parameters as regressors of no

interest to remove artificial correlations. The second-level statistics were assessed as in conventional analysis for contrast related to correlation with the seed region. Age and gender were used as covariates for between-group analyses. Correlation analysis between behavioural outcomes and seed functional connectivity in both groups was assessed and the effects of LED and disease duration were analysed for the PD group with age and gender as covariates. Group results were assessed using cluster-level inference at $p(\text{FWE}) < 0.05$ at a height threshold of $p(\text{uncor}) < 0.001$. The small volume correction on PCC was used in conventional analysis for the LED effect within the PD group in order to demarcate this region anatomically (using WFU-Pickatlas utility).

Analysis of resting-state fMRI data

The same pre-processing steps using SPM5 were made for the resting-state data: realignment and unwarping of functional scans, normalization to fit into a standard anatomical space (MNI), and spatial smoothing using a Gaussian filter with an FWHM of 8 mm. The voxel size generated from the above acquisition parameters was oversampled to $3 \times 3 \times 3$ mm. The group ICA toolbox GIFT (<http://icatb.sourceforge.net/>) (Calhoun et al. 2001) was used to perform independent component analysis. Subjects from the two groups (HC and PD) were put into the ICA together. The optimal number of components was chosen according to the minimum descriptive length criteria (Li et al. 2007). The intensity normalization was used prior to ICA analysis. No scaling of final components was used. Thus, the final components should represent the percent of the signal change. ICA was performed using the INFOMAX algorithm, and the GICA3 back-reconstruction algorithm was used to create individual subject components. The component related to the default mode system was chosen from the group of components using the DMN mask included in the GIFT program (Garrity et al. 2007). Corresponding individual subject's components from the ICA back-reconstruction process were selected to assess between-group effects in SPM5. The second-level statistics

were analysed the same way as in conventional analysis with covariates for the age and gender of subjects. Correlation analysis between behavioural outcomes and resting-state data in both groups was assessed and in the PD group the effect of daily LED and disease duration was also assessed with age and gender as covariates. Group results were assessed using cluster-level inference at $p(\text{FWE}) < 0.05$ at a height threshold of $p(\text{uncor}) < 0.001$. To compare not only spatial maps of DMN components but also spectral characteristics of the time series of these components, we used spectral comparison as implemented in GIFT.

Results

Behavioural data (see also Table 1)

All the participants in the HC and PD groups were non-demented with average results in the ACE-R of 94 ± 3.7 points and 94 ± 3.7 points, respectively (identical results in both groups).

Average results in the complex visual scene-encoding task (recognition tested; relative achievement in %) were $74 \pm 9.7\%$ for PD, and $91 \pm 9.0\%$ for HC. There was no significant difference between the results of the PD and HC groups ($p = 0.681$).

The Unified Parkinson’s Disease Rating Scale subscore V (the modified Hoehn–Yahr score assessing motor stage of PD; Fahn et al. 1987) ranged between 2 and 2.5, i.e. our patients had bilateral involvement without any major postural instability. All patients were examined in their on-medication state and the mean calculated LED in the PD group was 696 ± 430 mg/day. The magnitude of daily LED was not associated with cognitive outcomes (i.e. results of ACE-R, MMSE, and complex visual scene-encoding task performance). The average disease duration of PD as an indirect marker of

the disease severity was 4.44 ± 2.83 , the duration of treatment was 4.06 ± 2.96 . We observed no effect of disease duration on individual DMN analyses in the PD group.

Between-group analysis

Irrespective of the method used, we identified the involvement of the PCC/P, MPFC/ACC, insulae, inferior parietal lobules, angular gyri, supramarginal gyri, the superior and middle temporal gyri, precentral gyri, and middle frontal gyri (all bilaterally) within the DMN in both groups. In addition, caudate nuclei, postcentral gyri and superior frontal gyri bilaterally were engaged in deactivations in HC group while PD group deactivated only right caudate nucleus and right postcentral gyrus (see Table 2 for deactivations during a cognitive task performance). For MRI signal increases during the cognitive task, see Table 3. The patterns of activation were similar in both groups.

All three methods were used to evaluate the DMN in both groups, i.e. results of resting-state data using independent component analysis (Fig. 2a), results of the DMN as measured by deactivations during the complex visual scene-encoding task (Fig. 2b), and results of seed functional connectivity analyses (data extracted from deactivations during the complex visual scene-encoding task with seed placed in PCC/P and MD/FC/ACC) (Fig. 2c, d) did not reveal any significant differences when comparing the PD and HC groups ($p = 0.05$ corrected, cluster-level inference). We also did not find any correlation between the behavioural outcomes (ACE-R score and its all subscores including MMSE and recognition of complex visual scene-encoding task) and our resting-state data, deactivations/activations and seed functional connectivity. The comparison of spectral characteristics of the time series of DMN components from resting-state data did not reveal significant differences.

Table 1 Demographic and cognitive data

	HC				PD								
	Age	ACE	MMSE	CVSET	Age	DI	DT	LED	HY	UPDRS III	ACE	MMSE	CVSET
Average values	60.89	94.17	29.50	75.65	63.50	4.44	4.06	696	1.89	13.50	93.94	29.56	74.12
SD	6.67	3.49	0.71	7.48	9.07	2.83	2.96	430.35	0.44	5.31	3.67	0.78	9.70
Min	46	89	28	55.83	44	1	1	0	1	4	89	27	60.00
Max	77	100	30	88.33	84	9	9	1,500	2.5	24	100	30	90.00

ACE Addenbrooke’s Cognitive Examination (revised Czech version), MMSE mini-mental state examination, CVSET complex visual scene-encoding task (relative achievement in %), DI duration of illness (years), DT duration of treatment (years), HY Hoehn and Yahr score, UPDRS III Unified Parkinson’s Disease Rating Scale, subscore III, motor examination; LED daily levodopa-equivalent dose (mg/day)

Table 2 Brain deactivation during complex visual scene-encoding task

Cluster number	Cluster size	Region	x	y	z	T value	Z score
(a) Healthy controls							
#1	7,243 voxels	Precuneus/BA7 (left)	-6	-63	30	13.25	7.68
		Precuneus/BA7 (right)	6	-69	27	11.98	7.33
		Posterior cingulate gyrus (left)	0	-30	30	11.25	7.11
		Superior temporal gyrus/BA39 (right)	57	-57	21	11.75	7.26
		Angular gyrus (right)	48	-72	36	9.92	6.66
		Inferior parietal lobule/BA40 (right)	60	-39	33	8.48	6.09
		Inferior parietal lobule/BA40 (left)	-63	-39	24	11.01	7.03
		Middle temporal gyrus (left)	-54	-69	24	10.11	6.73
		Superior temporal gyrus (left)	-48	-60	18	9.71	6.58
		Middle temporal gyrus (right)	39	51	12	10.50	6.86
		Superior frontal gyrus/BA10 (right)	24	45	30	8.95	6.29
		Insula/BA13 (right)	51	-33	18	10.20	6.76
		Precentral gyrus (right)	54	0	12	9.59	6.54
		Superior frontal gyrus (left)	-33	48	18	9.71	6.58
		Middle frontal gyrus/BA9 (left)	-30	57	12	9.12	6.36
		Anterior cingulate cortex/BA24 (right)	3	21	27	8.95	6.29
		Medial frontal gyrus (right)	9	51	9	8.10	5.93
		Precentral gyrus (left)	-54	-9	9	8.62	6.16
		Postcentral gyrus (left)	-54	-12	24	8.34	6.04
		Insula/BA13 (left)	-42	-9	3	7.86	5.82
		Postcentral gyrus (right)	36	-21	30	5.83	4.78
		Anterior cingulate cortex/BA42 (left)	-9	45	12	8.09	5.93
		Medial frontal gyrus (left)	-6	54	15	6.70	5.26
		Posterior cingulate gyrus/BA23 (right)	6	-45	24	10.34	6.81
		Middle frontal gyrus/BA10 (right)	39	51	12	10.50	6.86
		Caudate nucleus (right)	16	12	15	6.00	4.88
		Supramarginal gyrus/BA40 (left)	-60	-51	30	9.17	6.38
		Supramarginal gyrus/BA40 (right)	57	-57	30	10.52	6.87
		Angular gyrus/BA39 (left)	-47	-72	33	7.27	5.55
		#2	42 voxels	Caudate nucleus (left)	-15	9	15
#3	17 voxels	Middle temporal gyrus (left)	-54	-30	0	6.81	5.32
(b) PD patients							
#1	3,112 voxels	Precuneus/BA7 (left)	-6	-63	30	12.67	7.53
		Precuneus (right)	12	-60	30	11.99	7.33
		Posterior cingulate gyrus (right)	6	-51	27	11.04	7.04
		Middle temporal gyrus/BA39 (left)	-54	-66	18	12.29	7.42
		Superior temporal gyrus/BA39 (left)	-42	-60	15	12.28	7.42
		Inferior parietal lobule/BA40 (left)	-63	-39	24	11.30	7.12
		Posterior cingulate gyrus/BA31 (left)	-3	-27	39	9.26	6.41
		Insula/BA13 (left)	-36	6	12	6.68	5.25
		Angular gyrus (left)	-48	-69	39	6.24	5.01
		Precentral gyrus/BA43 (left)	-54	-6	12	8.01	5.89
		Postcentral gyrus (left)	-63	-18	15	7.77	5.78
		Supramarginal gyrus/BA40 (left)	-63	-54	24	8.47	6.09
#2	1,891 voxels	Supramarginal gyrus/BA40 (right)	54	-54	21	12.36	7.44
		Insula/BA13 (right)	51	-33	18	10.42	6.83
		Superior temporal gyrus/BA22 (right)	57	6	6	9.91	6.65

Table 2 continued

Cluster number	Cluster size	Region	<i>x</i>	<i>y</i>	<i>z</i>	<i>T</i> value	<i>Z</i> score
#3	368 voxels	Middle temporal gyrus/BA39 (right)	51	-33	3	8.20	5.98
		Angular gyrus (right)	48	-69	30	9.32	6.44
		Precentral gyrus (right)	54	3	12	9.06	6.33
		Postcentral gyrus (right)	57	-15	15	9.06	6.33
		Inferior parietal lobule/BA40 (right)	57	-36	30	9.31	6.43
		Anterior cingulate gyrus/medial frontal gyrus (right)	3	27	24	8.69	6.19
		Anterior cingulate gyrus/BA24 (left)	-6	33	15	8.32	6.03
#4	92 voxels	Medial frontal gyrus (left)	-6	54	12	6.73	5.27
		Middle frontal gyrus/BA9 (left)	-27	30	33	7.73	5.76
#5	27 voxels	Caudate nucleus (left)	-15	6	15	6.74	5.28
#6	66 voxels	Middle frontal gyrus (right)	30	21	36	6.72	5.27

Evaluated on cluster-level inference $p < 0.05$, FWE corrected. Minimum cluster size 5 voxels

Effect of LED in the PD group

Functional connectivity analysis with seed in PCC/P and in MPFC/ACC

We found a significant positive effect of daily LED on the magnitude of functional connectivity within the PCC, i.e. the higher the LED, the higher the strength of correlation between the seed functional connectivity with the seed located in P/PCC and PCC itself (cluster peak at -15, -60, 3; cluster significance $p = 0.022$ FWE corrected, cluster size = 11 voxels, cluster-level inference with small volume correction using the PCC region as a mask) (Fig. 3). Spearman correlation coefficient at cluster peak was $r = 0.83$. We did not observe any significant correlation

between the LED and functional connectivity with the seed placed in MPFC/ACC.

Deactivation and activation during the complex visual scene-encoding task

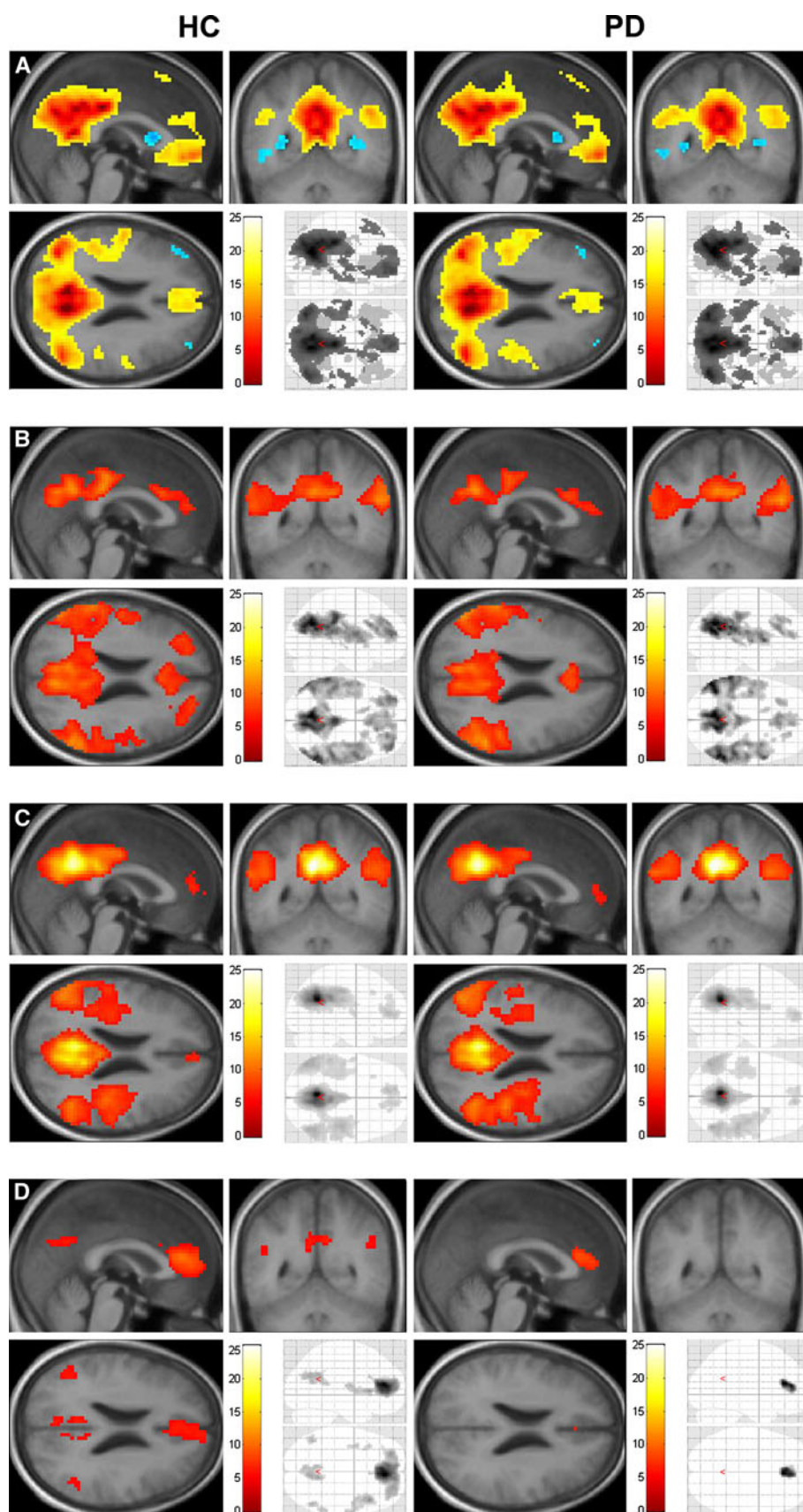
We did not find a direct effect of LED on deactivation in PD, but we found a negative correlation between daily LED and the magnitude of activation in the left parahippocampal gyrus (cluster peak at -21, -42, -9; cluster significance $p = 0.01$ FWE corrected, cluster size = 65 voxels; cluster-level inference), i.e. the higher the LED, the lower the activation in the left parahippocampal gyrus (Fig. 4). Spearman correlation coefficient at cluster peak was $r = 0.86$.

Table 3 Brain activation during complex visual scene-encoding task

Cluster number	Cluster size	Region	<i>x</i>	<i>y</i>	<i>z</i>	<i>T</i> value	<i>Z</i> score
(a) Healthy controls							
#1	1,368	Inferior occipital gyrus/lingual gyrus (left)	-33	-90	-9	15.59	8.16
		Fusiform gyrus/parahippocampal gyrus (left)	-30	-54	-12	14.55	8.00
		Middle occipital gyrus/BA18 (left)	-30	-93	0	14.46	7.98
		Middle occipital gyrus/BA18 (right)	36	-90	0	15.57	8.16
		Lingual gyrus/inferior occipital gyrus (right)	24	-93	-9	11.51	7.19
		Fusiform gyrus/parahippocampal gyrus (right)	36	-48	-12	11.20	7.09
(b) PD patients							
#1	2,090	Middle occipital gyrus/BA18 (right)	36	-90	0	18.07	8.29
		Inferior occipital gyrus/lingual gyrus (left)	-36	-87	-9	16.65	8.29
		Middle occipital gyrus/BA18 (left)	-30	-93	0	15.06	8.10
		Fusiform gyrus/parahippocampal gyrus (left)	-33	-51	-12	15.74	8.16
		Parahippocampal gyrus/BA37 (right)	33	-39	-12	12.30	7.42
		Fusiform gyrus (right)	36	-48	-12	11.93	7.32
		Inferior occipital gyrus/lingual gyrus (right)	12	-84	-12	12.42	7.46

Evaluated on cluster-level inference $p < 0.05$, FWE corrected. Minimum cluster size 5 voxels

Fig. 2 Brain regions engaged in DMN in both groups using all three methods of data processing ($p < 0.05$ FWE corrected). **a** ICA of resting state; **b** deactivation during the complex visual scene-encoding task; **c** functional connectivity from cognitive task data with seed located in PCC/P; **d** functional connectivity from cognitive task data with seed located in MPFC/ACC



Discussion

The goal of our study was to compare the integrity of the DMN in two groups of subjects: cognitively unimpaired PD patients on dopaminergic medication, and HC. In the PD group, we also assessed the influence of LED on the DMN and its functional connectivity. We did not find any significant difference in the DMN integrity between HC and PD as measured by ICA of the resting-state data, by BOLD signal decreases during the performance of a cognitive task, or by the seed functional connectivity with the seed located in the PCC/P or MPFC/ACC.

Previously described specific malfunctioning of the DMN in PD patients (Delaveau et al. 2010; Van Eimeren et al. 2009), as well as in cortico-striatal connectivity during the resting state (Helmich et al. 2010), was observed only under hypodopaminergic conditions. On the other hand, two studies evaluating the effect of an acute dopaminergic challenge to DMN integrity in PD patients (Delaveau et al. 2010; Nagano-Saito et al. 2009) demonstrated its positive effect. In the on-medication condition, the pattern of deactivations within the DMN was comparable to that of HC; this finding is in line with our results. More specifically, Nagano-Saito et al. (2009) showed in their H2 15O-PET study that modulation of dopamine function by the D1/D2 dopamine agonist apomorphine may improve performance on the Tower of London spatial planning task by increasing deactivation within the DMN in both the elderly HC and PD patients, resulting in similar DMN in both groups. The authors found greater correlation between task complexity and deactivation in the ventromedial prefrontal cortex (part of DMN) under apomorphine conditions in both the HC and PD groups. In the latter study (Delaveau et al. 2010), the brain deactivations were assessed using fMRI during a facial emotion recognition task. PD patients in hypodopaminergic condition (taking a placebo) deactivated only parts of the DMN as compared to HC, but after levodopa administration, the DMN integrity was restored. These findings imply that an acute challenge of dopaminergic medication has a relevant influence on DMN integrity in PD patients.

To further investigate whether the effect of a stable dopaminergic medication on the DMN is dose-dependent, we used correlation analyses between the daily LED and deactivation in the DMN and/or its functional connectivity. We found that the strength of functional connectivity within the DMN, specifically in the left PCC, was positively correlated with the magnitude of daily LED in our PD group while it was not correlated with the disease duration. Our results must be interpreted with caution since we only used correlation analyses in our PD patients on medication, and we did not compare ON- and OFF-medication conditions or different doses of LED in each subject.

The PCC, as one of the main nodes of the DMN, is connected to the hippocampus and linked to memory functions (Supekar et al. 2008; Wang et al. 2006). It is also known for its role in visuospatial orientation. Despite some evidence of a scarce dopaminergic innervation of the parietal cortices (Berger et al. 1988; Herrera-Marschitz et al. 1989), the indirect modulation of the precuneus by dopamine through thalamo-cortical pathways is more likely than its direct modulation (Tomasi et al. 2009).

While previous studies in PD populations showed that the dopaminergic challenge restored the deficits in deactivations or the connectivity within the DMN, Kelly et al. (2009) conversely demonstrated that levodopa reduced functional connectivity within the PCC and between the PCC and MPFC in young HC (mean age 26 years). In the same vein, Argyelan et al. (2008) reported that deactivations in the ventromedial prefrontal cortex during a motor sequence learning task in unmedicated PD patients were lost after an intravenous levodopa infusion. Age, baseline DMN integrity, and baseline cognitive performance may play a role. In addition, the inter-individual differences in the effect of dopamine challenge that reflect inter-individual differences in baseline dopamine levels may be important. U-shaped relationships between dopamine levels and fMRI/PET activation levels, and between dopamine levels and behavioural performance have been hypothesized (Cools 2006; Cools et al. 2009; Kelly et al. 2009; Rowe et al. 2008). Finally, the influence of genotype has also been suggested (Argyelan et al. 2008).

In our study we also found a significant negative correlation between daily LED and MR signal increases in the left parahippocampal gyrus during performance of the cognitive task. In other words, with the higher daily LED we observed lower activation in the left parahippocampal gyrus.

The hippocampus and parahippocampal gyrus are the structures typically involved in memory processes. Activation of the hippocampal formation has been well described during the performance of various cognitive tasks, especially when related to memory functions, including our complex visual scene-encoding task (Dickerson et al. 2005; Rabin et al. 2004; Shohamy and Adcock 2010; Spreng and Grady 2010). But the hippocampus is also engaged in non-mnemonic processes, such as pure visual discrimination of scenes (Davies et al. 2004), which has also been implicated in our task. There is evidence for both the dopaminergic innervation of the hippocampus (Bohnen et al. 2008; Navailles et al. 2010; Roggenhofer et al. 2010) and its connection with the mesocortical limbic circuitry. Since the mesocortical dopaminergic system is disrupted in PD (Javoy-Agid and Agid 1980; Mattay et al. 2002), it is not that surprising that the magnitude of daily LED was related to MRI signal changes specifically in the

Fig. 3 Positive effect of LED on the DMN functional connectivity in the PCC-PD group ($p < 0.022$ FWE, cluster-level inference, small volume correction using the PCC region as a mask)

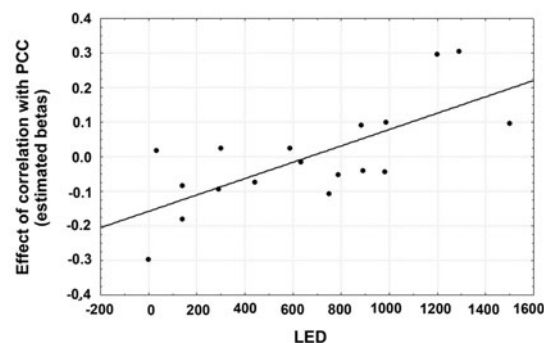
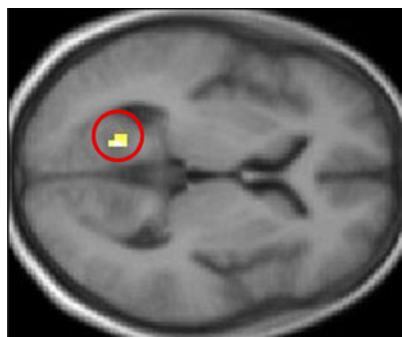
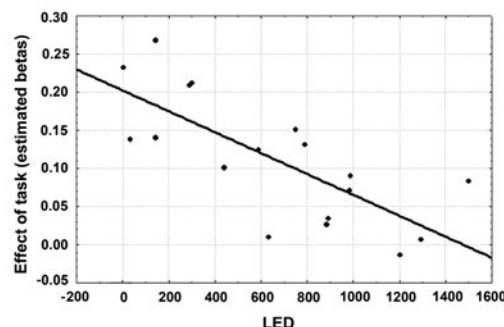
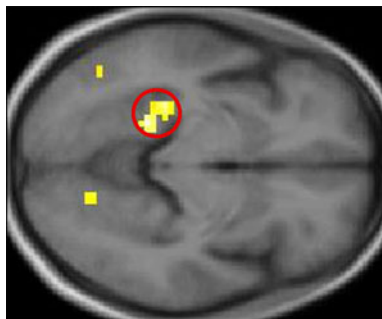


Fig. 4 Negative correlation between LED and activation in the left parahippocampal gyrus-PD group ($p < 0.05$ FWE, cluster-level inference)



left parahippocampal gyrus during the cognitive task performance. Similar “focusing” effects of dopamine on functional brain imaging patterns have already been shown by others (for review, see Cools 2006; Ng et al. 2010). For example, Mattay et al. (2002) demonstrated that the cortical regions subserving working memory displayed greater activation during the hypodopaminergic state compared to the on-medication condition. These fMRI changes were accompanied by behavioural effects, i.e. improvement of the performance whilst on medication. In our study, the tested cognitive performance was not correlated with either the daily LED or with the LED-induced variability of BOLD signal changes in the left parahippocampal gyrus. This inconsistency could have been caused by the possible “ceiling” effect (PD patients were cognitively intact when tested on medication) and by the low inter-individual variability of cognitive outcomes (making the correlation analysis difficult). We did not compare the ON- and OFF-medication conditions, and therefore direct comparisons with the results of the study by Mattay et al. (2002) cannot be made.

Conclusion

We did not find any significant differences in the DMN integrity between cognitively normal PD patients on dopaminergic medication and HC. We extended the recent knowledge about the role of dopamine in modulation of the

DMN in the PD population by showing that this effect seems to be dose-dependent. We demonstrated the influence of the daily dose of stable dopaminergic medication on both the magnitude of functional connectivity within the DMN and the task-related MRI signal increases, i.e. on both task-positive and task-negative large-scale brain networks. Further studies are needed to confirm our results on a larger PD sample size and to test different doses of dopaminergic drugs.

References

- Achard S, Bullmore E (2007) Efficiency and cost of economical brain functional networks. *PLoS Comput Biol* 3:e17
- Argyelan M, Carbon M, Ghilardi MF, Feigin A, Mattis P, Tang C, Dhawan V, Eidelberg D (2008) Dopaminergic suppression of brain deactivation responses during sequence learning. *J Neurosci* 28:10687–10695
- Berger B, Trottier S, Verney C, Gaspar P, Alvarez C (1988) Regional and laminar distribution of the dopamine and serotonin innervation in the macaque cerebral cortex: a radioautographic study. *J Comp Neurol* 273:99–119
- Binder JR, Frost JA, Hammeke TA, Bellgowan PS, Rao SM, Cox RW (1999) Conceptual processing during the conscious resting state. A functional MRI study. *J Cogn Neurosci* 11:80–95
- Bluhm RL, Miller J, Lanius RA, Osuch EA, Boksman K, Neufeld RW, Théberge J, Schaefer B, Williamson P (2007) Spontaneous low-frequency fluctuations in the BOLD signal in schizophrenic patients: anomalies in the default network. *Schizophr Bull* 33:1004–1012
- Bohnen NI, Gedela S, Herath P, Constantine GM, Moore RY (2008) Selective hyposmia in Parkinson disease: association with hippocampal dopamine activity. *Neurosci Lett* 447:12–16

- Broyd SJ, Demanuele C, Debener S, Helps SK, James CJ, Sonuga-Barke EJ (2009) Default-mode brain dysfunction in mental disorders: a systematic review. *Neurosci Biobehav Rev* 33:279–296
- Buckner RL, Snyder AZ, Shannon BJ, LaRossa G, Sachs R, Fotenos AF, Sheline YI, Klunk WE, Mathis CA, Morris JC, Mintun MA (2005) Molecular, structural, and functional characterization of Alzheimer's disease: evidence for a relationship between default activity, amyloid, and memory. *J Neurosci* 25:7709–7717
- Calhoun VD, Adali T, Pearlson GD, Pekar JJ (2001) A method for making group inferences from functional MRI data using independent component analysis. *Hum Brain Map* 14:140–151
- Cools R (2006) Dopaminergic modulation of cognitive function—implications for L-DOPA treatment in Parkinson's disease. *Neurosci Biobehav Rev* 30:1–23
- Cools R, Frank MJ, Gibbs SE, Miyakawa A, Jagust W, D'Esposito M (2009) Striatal dopamine predicts outcome-specific reversal learning and its sensitivity to dopaminergic drug administration. *J Neurosci* 29:1538–1543
- Davies RR, Graham KS, Xuereb JH, Williams GB, Hodges JR (2004) The human perirhinal cortex and semantic memory. *Eur J Neurosci* 20:2441–2446
- Delaveau P, Salgado-Pineda P, Fossati P, Witjas T, Azulay JP, Blin O (2010) Dopaminergic modulation of the default mode network in Parkinson's disease. *Eur Neuropsychopharmacol* 20:784–792
- Dickerson BC, Salat DH, Greve DN, Chua EF, Rand-Giovannetti E, Rentz DM, Bertram L, Mullin K, Tanzi RE, Blackner D, Albert MS, Sperling RA (2005) Increased hippocampal activation in mild cognitive impairment compared to normal aging and AD. *Neurology* 65:404–411
- Fahn S, Elston RL, members of the UPDRS Development Committee (1987) Unified Parkinson's disease rating scale. In: Fahn S, Marsden CD, Goldstein M, Calne DB (eds) Recent developments in Parkinson's disease, vol 2. MacMillan, New York, pp 53–163
- Fox MD, Raichle ME (2007) Spontaneous fluctuations in brain activity observed with functional magnetic resonance imaging. *Nat Rev Neurosci* 8:700–711
- Fox MD, Snyder AZ, Vincent JL, Corbetta M, Van Essen DC, Raichle ME (2005) The human brain is intrinsically organized into dynamic, anticorrelated functional networks. *Proc Natl Acad Sci USA* 102:9673–9678
- Garrity AG, Pearlson GD, McKiernan K, Lloyd D, Kiehl KA, Calhoun VD (2007) Aberrant “default mode” functional connectivity in schizophrenia. *Am J Psychiatry* 164:450–457
- Greicius MD, Srivastava G, Reiss AL, Menon V (2004) Default-mode network activity distinguishes Alzheimer's disease from healthy aging: evidence from functional MRI. *Proc Natl Acad Sci USA* 101:4637–4642
- Gusnard DA, Raichle ME, Raichle ME (2001) Searching for a baseline: functional imaging and the resting human brain. *Nat Rev Neurosci* 2:685–694
- Helmich RC, Derikx LC, Bakker M, Scheeringa R, Bloem BR, Toni I (2010) Spatial remapping of cortico-striatal connectivity in Parkinson's disease. *Cereb Cortex* 20:1175–1186
- Herrera-Marschitz M, Gojny M, Utsumi H, Ungerstedt U (1989) Mesencephalic dopamine innervation of the frontoparietal (sensorimotor) cortex of the rat: a microdialysis study. *Neurosci Lett* 97:266–270
- Hughes AJ, Daniel SE, Kilford L, Lees AJ (1992) Accuracy of clinical diagnosis of idiopathic Parkinson's disease: a clinicopathological study of 100 cases. *J Neurol Neurosurg Psychiatry* 55:181–184
- Hummelová-Fanfrdlová Z, Rektorová I, Sheardová K, Bartoš A, Línec V, Rössner P, Zapletalová J, Vyhnanek M, Hort J (2009) Česká adaptace Addenbrookského kognitivního testu. *Československá psychologie* 53:376–388
- Javoy-Agid F, Agid Y (1980) Is the mesocortical dopaminergic system involved in Parkinson's disease? *Neurology* 30:1326–1330
- Kelly C, De Zubicaray G, Di Martino A, Copland DA, Reiss PT, Klein DF, Castellanos FX, Milham MP, McMahon K (2009) L-Dopa modulates functional connectivity in striatal cognitive and motor networks: a double-blind placebo controlled study. *J Neurosci* 29:7364–7378
- Krajcovicova L, Mikl M, Marecek R, Rektorova I (2010) Default mode network analysis in healthy controls (pilot study). *Cesk Slov Neurol N* 73:517–232
- Li SJ, Biswal B, Li Z, Risinger R, Rainey C, Cho JK, Salmeron BJ, Stein EA (2000) Cocaine administration decreases functional connectivity in human primary visual and motor cortex as detected by functional MRI. *Magn Reson Med* 43:45–51
- Li SJ, Li Z, Wu G, Zhang MJ, Franczak M, Antuono PG (2002) Alzheimer disease: evaluation of a functional MR imaging index as a marker. *Radiology* 225:253–259
- Li Y, Adali T, Calhoun VD (2007) Estimating the number of independent components for functional magnetic resonance imaging data. *Hum Brain Mapp* 28:1251–1266
- Liang M, Zhou Y, Jiang T, Liu Z, Tian L, Liu H, Hao Y (2006) Widespread functional disconnectivity in schizophrenia with resting-state functional magnetic resonance imaging. *Neuroreport* 17:209–213
- Liu Y, Wang K, Yu C, He Y, Zhou Y, Liang M, Wang L, Jiang T (2008) Regional homogeneity, functional connectivity and imaging markers of Alzheimer's disease: a review of resting-state fMRI studies. *Neuropsychologia* 46:1648–1656
- Mathuranath PS, Nestor PJ, Berrios GE, Rakowicz W, Hodges JR (2000) A brief cognitive test battery to differentiate Alzheimer's disease and frontotemporal dementia. *Neurology* 55:1613–1620
- Mattay VS, Tessitore A, Callicott JH, Bertolino A, Goldberg TE, Chase TN, Hyde TM, Weinberger DR (2002) Dopaminergic modulation of cortical function in patients with Parkinson's disease. *Ann Neurol* 51:156–164
- Nagano-Saito A, Leyton M, Monchi O, Goldberg YK, He Y, Dagher A (2008) Dopamine depletion impairs frontostriatal functional connectivity during a set-shifting task. *J Neurosci* 28(14):3697–3706
- Nagano-Saito A, Liu J, Doyon J, Dagher A (2009) Dopamine modulates default mode network deactivation in elderly individuals during Tower of London task. *Neurosci Lett* 458:1–5
- Navailles S, Benazzou A, Bioulac B, Gross C, De Deurwaerdère P (2010) High-frequency stimulation of the subthalamic nucleus and L-3, 4-dihydroxyphenylalanine inhibit in vivo serotonin release in the prefrontal cortex and hippocampus in a rat model of Parkinson's disease. *J Neurosci* 30:2356–2364
- Ng B, Palmer S, Abugharbieh R, McKeown MJ (2010) Focusing effects of L-dopa in Parkinson's disease. *Hum Brain Mapp* 31:88–97
- Parkin SG, Gregory RP, Scott R, Bain P, Silburn P, Hall B, Boyle R, Joint C, Aziz TZ (2002) Unilateral and bilateral pallidotomy for idiopathic Parkinson's disease: a case series of 115 patients. *Mov Disord* 17:682–692
- Rabin ML, Narayan VM, Kimberg DY, Casasanto DJ, Glosser G, Tracy JL, French JA, Sperling MR, Detre JA (2004) Functional MRI predicts post-surgical memory following temporal lobectomy. *Brain* 127:2286–2298
- Raichle ME, Snyder AZ (2007) A default mode of brain function: a brief history of an evolving idea. *Neuroimage* 37:1083–1090
- Raichle ME, MacLeod AM, Snyder AZ, Powers WJ, Gusnard DA, Shulman GL (2001) A default mode of brain function. *Proc Natl Acad Sci USA* 98:676–682
- Robinson S, Basso G, Soldati N, Sailer U, Jovicich L, Bruzzone L, Krayspin-Exner I, Bauer H, Moser E (2009) A resting state

- network in the motor control circuit of the basal ganglia. *BMC Neurosci* 10:137
- Rogers BP, Morgan VL, Newton AT, Gore JC (2007) Assessing functional connectivity in the human brain by fMRI. *Magn Reson Imaging* 25:1347–1357
- Roggenhofer E, Fidzinski P, Bartsch J, Kurz F, Shor O, Behr J (2010) Activation of dopamine D1/D5 receptors facilitates the induction of presynaptic long-term potentiation at hippocampal output synapses. *Eur J Neurosci* 32:598–605
- Rowe JB, Hughes L, Ghosh BC, Eckstein D, Williams-Gray CH, Fallon S, Barker RA, Owen AM (2008) Parkinson's disease and dopaminergic therapy—differential effects on movement, reward and cognition. *Brain* 131:2094–2105
- Shohamy D, Adcock RA (2010) Dopamine and adaptive memory. *Trends Cogn Sci* 14:464–472
- Spreng RN, Grady CL (2010) Patterns of brain activity supporting autobiographical memory, prospection, and theory of mind, and their relationship to the default mode network. *J Cogn Neurosci* 22:1112–1123
- Supekar K, Menon V, Rubin D, Musen M, Greicius MD (2008) Network analysis of intrinsic functional brain connectivity in Alzheimer's disease. *PLoS Comput Biol* 4:e1000100
- Tomasi D, Volkow ND, Wang R, Telang F, Wang G, Chang L, Ernst T, Fowler JS (2009) Dopamine transporters in striatum correlate with deactivation in the default mode network during visuospatial attention. *PLoS One* 4:e6102
- Van Eimeren T, Monchi O, Ballanger B, Straffella AP (2009) Dysfunction of the default mode network in Parkinson disease. *Arch Neurol* 66:877–883
- Wang L, Zang Y, He Y, Liang M, Zhang X, Tian L, Wu T, Jiang T, Li K (2006) Changes in hippocampal connectivity in the early stages of Alzheimer's disease: evidence from resting state fMRI. *Neuroimage* 31:496–504
- Weissenbacher A, Kasess C, Gerstl F, Lanzenberger R, Moser E, Windischberger C (2009) Correlations and anticorrelations in resting-state functional connectivity MRI: a quantitative comparison of preprocessing strategies. *Neuroimage* 47:1408–1416
- World Health Organization (2007) International statistical classification of diseases and related health problems, 10th revision. Version for 2007. World Health Organization (<http://apps.who.int/classifications/apps/icd/icd10online/>)
- Zang YF, He Y, Zhu CZ, Cao QJ, Sui MQ, Liang M, Tian LX, Jiang TZ, Wang YF (2007) Altered baseline brain activity in children with ADHD revealed by resting-state functional MRI. *Brain Dev* 29:83–91
- Zhou Y, Liang M, Jiang T, Tian L, Liu Y, Liu Z, Liu H, Kuang F (2007) Functional dysconnectivity of the dorsolateral prefrontal cortex in first-episode schizophrenia using resting-state fMRI. *Neurosci Lett* 417:297–302
- Zhou Y, Shu N, Liu Y, Song M, Hao Y, Liu H, Yu C, Liu Z, Jiang T (2008) Altered resting-state functional connectivity and anatomical connectivity of hippocampus in schizophrenia. *Schizophr Res* 100:120–132